A Generalized Analysis of Three-Dimensional Anisotropic Scattering in Mobile Wireless Channels-Part II: Second-Order Statistical Characterization

Petros Karadimas[(1)] and Jie Zhang[(2)]
[(1)] Centre for Wireless Research, Department of Computer Science and Technology, University of Bedfordshire, UK
[(2)]Centre for Wireless Network Design, Department of Electronic and Electrical Engineering, University of Sheffield, UK

***Abstract* - In a recent paper [1], we presented a generalized theoretical analysis for the diffuse multipath power in mobile wireless channels accounting for three-dimensional (3-D) multi-modal (i.e., clustered) scattering. In this paper, a parameterized case-study stemming from [1] is analyzed with multi-modal arrival of diffuse multipath power within four angular sectors. Those sectors are parametrically defined with respect to the mobile receiver's direction of motion. One sector per each quadrant is considered and the parametric probability density function (PDF) of the angle of arrival (AOA) is derived. From this PDF, the second order statistics of mobile channels with multi-modal scattering are derived, namely, the temporal autocorrelation function (ACF), the power spectral density (PSD), or Doppler spectrum, the level crossing rate (LCR) and average fade duration (AFD). Extension to generalized multi-modal arrival within any arbitrary number of angular sectors can be treated similarly.**

I. INTRODUCTION

Numerous statistical models are applicable for the angle of arrival (AOA) of diffuse multipath power in three-dimensional (3-D) scattering environments (see [1] and related references therein). From the probability density function (PDF) of AOA, we can end up to the second-order statistics of mobile wireless channels, namely, the temporal autocorrelation function (ACF), the power spectral density (PSD), or Doppler spectrum, the level crossing rate (LCR) and average fades duration (AFD) [2], [3].

The subject of this paper is to derive the second-order statistics of mobile wireless channels by using the recently developed statistical model presented in [1], which considered portions of diffuse multipath power to be allocated to discrete angular sectors. The multipath power within each sector was weighted by a positive-valued factor. With such modeling, any 3-D anisotropic scattering scenario can be theoretically treated by considering elemental weighted contributions from discrete sectors. Thus, flexible models suitable for a great range of wireless environments can be created. This paper completes the analysis of [1] by presenting a generic parameterized case-study. More specifically, the arrival of diffuse multipath power is confined within four discrete angular sectors, where one sector per quadrant is considered. Each sector is parametrically weighted in order to account for non-uniform portioning of multipath power. The sectors are appropriately defined such that the impact on the second-order statistics of any arbitrary number of sectors to be handled similarly. From the AOA PDF, the ACF is derived first. Then, the PSD is analytically derived after Fourier transforming the ACF. The LCR and AFD arise from formulas that contain values of the ACF and its derivatives at zero temporal difference.

Analytical derivation of PSD in mobile wireless channels has always been an intriguing issue especially for 3-D scattering scenarios. In [4], an analytical PSD was presented for a uniform 3-D scattering scenario truncated to a maximum symmetrical elevation AOA with respect to the azimuth plane. In [5], the PSD was calculated for purely 3-D isotropic scattering, thus constituting a special case of the PSD in [4]. In [6], a non-analytical expression for the PSD was presented by considering an alternative elevation AOA PDF with respect to that in [4]. In [7] and [8], the PSD was analytically derived for 3-D scattering scenarios, where the elevation AOA PDF was modeled by a family of sinusoidal functions [7] and a function combining sinusoids and exponentials [8]. The models [4]-[8] have in common that a uniform PDF for the azimuth AOA was considered. A non-analytical expression for the PSD can be seen in [9], where both the azimuth and elevation AOA PDFs follow a truncated uniform distribution. In [4]-[9], unimodal arrival was considered (i.e., arrival within one sector). The PSD was analytically calculated in [10] and [11] for 3-D scattering environments with bimodal arrival of multipath power (i.e., arrival within two discrete sectors). The elevation AOA was similar in both sectors with that in [4] and independent from the azimuth AOA. A theoretical model for the impact of receiving antenna pattern on the PSD in 3-D scattering environments was presented in [12]. Measurement campaigns in [13] and [14] showed PSDs arisen from 3-D multipath scattering.

The remaining second-order statistics, i.e., the LCR and AFD, give a qualitative description of the temporal variations of the received signal. Their importance is well-known for a variety of applications, such as determining the frame length for coded systems [15] and estimating the throughput of communication protocols [16]. They are determined by following similar formulations as in references [2], [3], [10] and [11].

The remaining of this paper is organized as follows. Section II presents the parameterized case-study with four discrete sectors of arrival. In Section III, the PSD is analytically derived for the aforementioned case-study after Fourier-transforming the ACF. The determination of the LCR and AFD follows from formulas containing values of the ACF and its derivatives at

978-1-4673-1881-5/12/$31.00 ©2012 IEEE

zero temporal difference. Finally, Section IV concludes this paper with a synopsis of the main results and advantages of the presented analysis.

II. THE PARAMETERIZED CASE-STUDY

We assume that the mobile receiver moves in the positive Y axis and diffuse multipath power arrives within four sectors, namely, S1: $a_{\min 1} \le a \le a_{\max 1}$ and $\beta_{\min 1} \le \beta \le \beta_{\max 1}$, S2: $\pi - a_{\max 2} \le a \le \pi - a_{\min 2}$ and $\beta_{\min 2} \le \beta \le \beta_{\max 2}$, S3: $-a_{\max 3} \le a \le -a_{\min 3}$ and $\beta_{\min 3} \le \beta \le \beta_{\max 3}$, S4: $-\pi + a_{\min 4} \le a \le -\pi + a_{\max 4}$ and $\beta_{\min 4} \le \beta \le \beta_{\max 4}$. The geometry of this case-study is depicted in Fig. 1. Details on the usefulness of such a modeling approach can be viewed in [1]. We have considered one sector per each quadrant because the PSD and ACF are determined by different formulations in each of them. Alternatively, if we had considered only one sector, we should have analyzed four different case studies based on which quadrant multipath power arrives. a is the azimuth AOA, which counts from the value $a = -\pi$ in the negative Y axis returning to the same point in the clockwise direction for $a = \pi$. $a_{\min i}$ and $a_{\max i}$, $(i = 1,2,3,4)$, are the minimum and maximum azimuth AOA in each sector, respectively, i.e., $0 \le a_{\min i} \le a_{\max i} \le \pi/2$. Fig. 2 graphically presents $a_{\min i}$ and $a_{\max i}$ by showing the projection of multimodal arrival of Fig. 1 onto the XY plane. β is the elevation AOA defined as $\beta = 0$ on the XY plane (the plane the receiver moves), $\beta = \pi/2$ on the positive Z axis and $\beta = -\pi/2$ on the negative Z axis. $\beta_{\min i}$ and $\beta_{\max i}$, $(i = 1,2,3,4)$, are the minimum and maximum elevation AOA in each sector, respectively, i.e., $0 \le |\beta_{\min i}| \le |\beta_{\max i}| \le \pi/2$. In this paper, we consider only a positive-valued elevation AOA, i.e., $0 \le \beta_{\min i} \le \beta \le \beta_{\max i} \le \pi/2$. In the next Section, it will be shown that with such definitions of the margins in each sector, generalized multi-modal arrival within any arbitrary number of angular sectors can be treated similarly.

Assuming S_i, $(i = 1,2,3,4)$, to be positive-valued weighting factors accounting for the contribution of sector i to the total received power, the joint azimuth and elevation AOA PDF, $p_{a,\beta}(a,\beta)$, will be [1]

$$p_{a,\beta}(a,\beta) = \begin{cases} S_1 U \cos\beta, & a,\ \beta \in \text{S1} \\ S_2 U \cos\beta, & a,\ \beta \in \text{S2} \\ S_3 U \cos\beta, & a,\ \beta \in \text{S3} \\ S_4 U \cos\beta, & a,\ \beta \in \text{S4} \\ 0, & otherwise \end{cases} \quad (1)$$

where U is a constant defined as

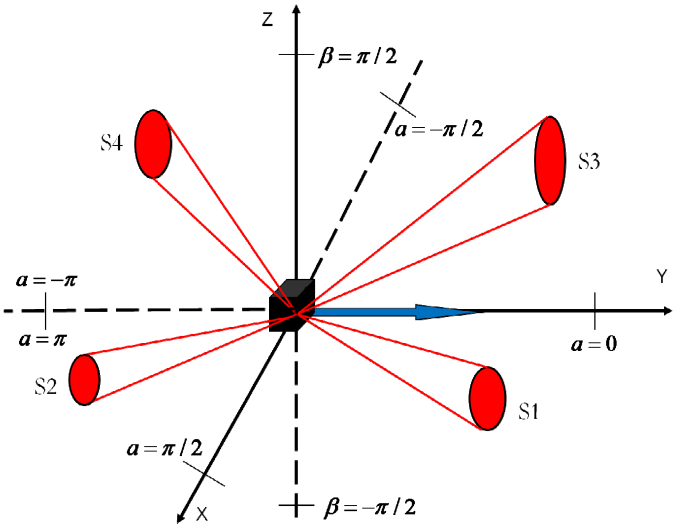

Fig. 1. Geometry of the parameterized case-study.

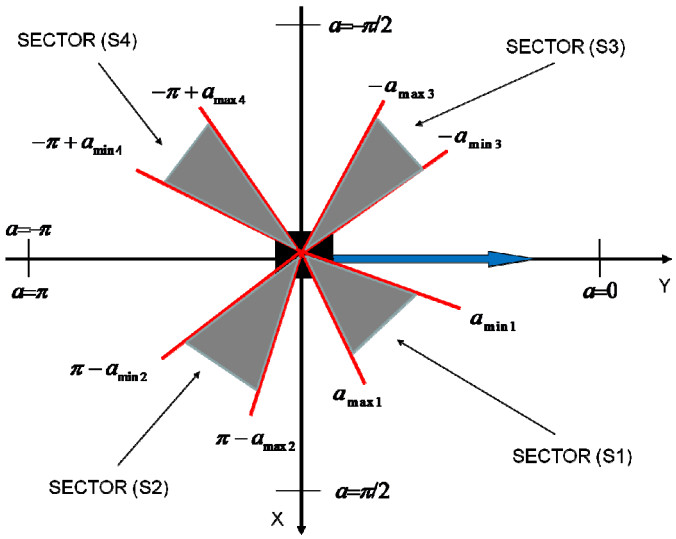

Fig. 2. Sectors of arrival on the azimuth XY plane.

$$U = \frac{1}{\sum_{i=1}^{4}[(\sin\beta_{\max i} - \sin\beta_{\min i})(a_{\max i} - a_{\min i})]}. \quad (2)$$

In order equation (1) to represent a valid PDF the following condition should hold for S_i, $(i = 1,2,3,4)$, [1]

$$\sum_{i=1}^{4}[S_i(\sin\beta_{\max i} - \sin\beta_{\min i})(a_{\max i} - a_{\min i})] = 1/U. \quad (3)$$

III. SECOND-ORDER STATISTICS

The ACF, $R_d(\tau)$, arisen from diffuse multipath power will be [11][1]

$$R_d(\tau) = 2\sigma^2 \iint \exp(j2\pi f_{\max}\tau\cos\beta\cos\alpha)\, p_{\alpha,\beta}(\alpha,\beta)\, d\alpha\, d\beta \quad (4)$$

[1] It is implied that the integral limits, when not given, cover the entire range of integration of the integrated variables.

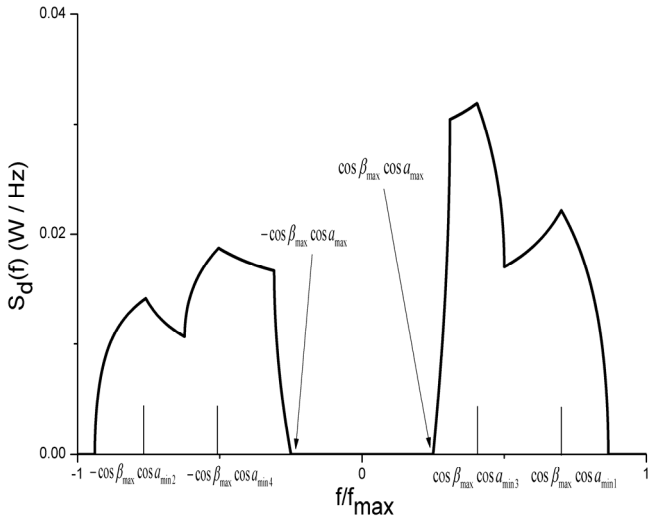

Fig. 3. PSD of the parameterized case-study (eq. (10)).

where τ is the difference between two temporal instants, $2\sigma^2$ is the mean diffuse multipath power and $f_{\max} = vf_0 / c$ is the maximum Doppler frequency shift, with v the mobile unit speed, c the speed of light in free space and f_0 the carrier frequency. Substituting equation (1) in equation (4), we take the ACF as follows

$$R_d(\tau) = J_1(\tau) + J_2(\tau) + J_3(\tau) + J_4(\tau) \quad (5)$$

where

$$J_1(\tau) = 2\sigma^2 S_1 U \times \int_{\beta_{\min 1}}^{\beta_{\min 2}} \int_{a_{\min 1}}^{a_{\max 1}} \cos\beta \exp(j2\pi f_{\max}\tau\cos\beta\cos a)\,da\,d\beta \quad (6)$$

$$J_2(\tau) = 2\sigma^2 S_2 U \times \int_{\beta_{\min 2}}^{\beta_{\max 2}} \int_{a_{\min 2}}^{a_{\max 2}} \cos\beta \exp(-j2\pi f_{\max}\tau\cos\beta\cos a)\,da\,d\beta \quad (7)$$

$$J_3(\tau) = J_1(\tau)\Big|_{a_{\min 1}\to a_{\min 3}, a_{\max 1}\to a_{\max 3}, \beta_{\min 1}\to\beta_{\min 3}, \beta_{\max 1}\to\beta_{\max 3}, S_1\to S_3} \quad (8)$$

$$J_4(\tau) = J_2(\tau)\Big|_{a_{\min 2}\to a_{\min 4}, a_{\max 2}\to a_{\max 4}, \beta_{\min 2}\to\beta_{\min 4}, \beta_{\max 2}\to\beta_{\max 4}, S_2\to S_4} \quad (9)$$

By Fourier transforming equation (5), we find the PSD, $S_d(f)$, as follows

$$S_d(f) = F[J_1(\tau)] + F[J_2(\tau)] + F[J_3(\tau)] + F[J_4(\tau)] \quad (10)$$

where $F[.]$ is the Fourier transform operator transforming the field of temporal difference τ into that of Doppler frequency shift f. The Fourier transforms in equation (10) are analytically solved as follows (see Appendix A)

$$F[J_1(\tau)] = \sigma^2 S_1 U / f_{\max} \times$$

$$\begin{cases} \text{a}rc\sin\dfrac{f^2(\sin^2 a_{\max 1}+1) - {f_{\max}}^2\cos^2 a_{\max 1}}{({f_{\max}}^2 - f^2)\cos^2 a_{\max 1}} - \\ \text{a}rc\sin\dfrac{f^2(\sin^2 a_{\min 1}+1) - {f_{\max}}^2\cos^2 a_{\min 1}}{({f_{\max}}^2 - f^2)\cos^2 a_{\min 1}}, \\ f_{\max}\cos a_{\min 1}\cos\beta_{\max 1} \le f \le f_{\max}\cos a_{\max 1}\cos\beta_{\min 1} \\ \text{a}rc\sin\dfrac{{f_{\max}}^2\cos(2\beta_{\min 1}) - f^2}{{f_{\max}}^2 - f^2} - \\ \text{a}rc\sin\dfrac{f^2(\sin^2 a_{\min 1}+1) - {f_{\max}}^2\cos^2 a_{\min 1}}{({f_{\max}}^2 - f^2)\cos^2 a_{\min 1}}, \\ \max\left(f_{\max}\cos a_{\min 1}\cos\beta_{\max 1}, f_{\max}\cos a_{\max 1}\cos\beta_{\min 1}\right) \le \\ f \le f_{\max}\cos a_{\min 1}\cos\beta_{\min 1} \\ \text{a}rc\sin\dfrac{f^2(\sin^2 a_{\max 1}+1) - {f_{\max}}^2\cos^2 a_{\max 1}}{({f_{\max}}^2 - f^2)\cos^2 a_{\max 1}} - \\ \text{a}rc\sin\dfrac{{f_{\max}}^2\cos(2\beta_{\max 1}) - f^2}{{f_{\max}}^2 - f^2}, \\ f_{\max}\cos a_{\max 1}\cos\beta_{\max 1} \le f \le \\ \min(f_{\max}\cos a_{\min 1}\cos\beta_{\max 1}, f_{\max}\cos a_{\max 1}\cos\beta_{\min 1}) \\ \text{a}rc\sin\dfrac{{f_{\max}}^2\cos(2\beta_{\min 1}) - f^2}{{f_{\max}}^2 - f^2} - \text{a}rc\sin\dfrac{{f_{\max}}^2\cos(2\beta_{\max 1}) - f^2}{{f_{\max}}^2 - f^2}, \\ f_{\max}\cos a_{\max 1}\cos\beta_{\min 1} \le f \le f_{\max}\cos a_{\min 1}\cos\beta_{\max 1} \\ 0, otherwise \end{cases} \quad (11)$$

$$F[J_2(\tau)] = F[J_1(\tau)]\Big|_{f\to -f, a_{\min 1}\to a_{\min 2}, a_{\max 1}\to a_{\max 2}, \beta_{\min 1}\to\beta_{\min 2}, \beta_{\max 1}\to\beta_{\max 2}, S_1\to S_2} \quad (12)$$

$$F[J_3(\tau)] = F[J_1(\tau)]\Big|_{a_{\min 1}\to a_{\min 3}, a_{\max 1}\to a_{\max 3}, \beta_{\min 1}\to\beta_{\min 3}, \beta_{\max 1}\to\beta_{\max 3}, S_1\to S_3} \quad (13)$$

$$F[J_4(\tau)] = F[J_2(\tau)]\Big|_{a_{\min 2}\to a_{\min 4}, a_{\max 2}\to a_{\max 4}, \beta_{\min 2}\to\beta_{\min 4}, \beta_{\max 2}\to\beta_{\max 4}, S_2\to S_4} \quad (14)$$

The usefulness of the above formulation of each sector (see Figs. 1 and 2) now becomes evident from equations (5)-(14). The impact of all sectors is determined following a similar approach with that of only one sector. Arbitrary number of angular sectors in each quadrant can be treated similarly too. Moreover, due to the even symmetry of cosine function, negative elevation AOAs are treated similarly with positive elevation AOAs. Using also the valid approximation $R_e(\tau) \approx |R_d(\tau)|^2$ [17], we can further determine the whole envelope correlation function $R_e(\tau)$ and not just the main lobe as in [18].

Fig. 3 shows the PSD for the following parameter set: $\beta_{\min i} = \beta_{\min} = 0$, $\beta_{\max i} = \beta_{\max} = \pi/5$, $a_{\max i} = a_{\max} = \pi/2.5$, $(i = 1,2,3,4)$, $a_{\min 1} = \pi/6$, $a_{\min 2} = \pi/9$, $a_{\min 3} = \pi/3$, $a_{\min 4} = \pi/3.5$, $f_{\max} = 91Hz$, $\sigma = 1$, $S_1 = S_3 = 1.35$ and $S_2 = S_4 = 0.74$. As it can be seen, the

PSD is discontinuous and asymmetric, with these properties being strongly dependent on the parameters of the AOA PDF.

Next, the LCR, $N(z)$, is defined as the average number of crossings per second that the received signal envelope crosses a specified level, z, with positive slope. In this paper, we consider that multipath power is purely diffuse with no existence of specular components. Thus, the number of multipath components is large and the central limit theorem (CLT) applies resulting a Rayleigh distributed envelope [19]. Accordingly, the LCR will be [2]

$$N(z) = \sqrt{b/(2\pi)}\exp[-z^2/(2\psi_0)]\cdot z/\psi_0 . \quad (15)$$

The AFD, $T(z)$, determines the mean value of the time intervals that the received signal envelope remains below a specified signal level z. With a Rayleigh distributed envelope, the AFD will be [2]

$$T(z) = \sqrt{(2\pi)/b}\{\exp[z^2/(2\psi_0)]-1\}\cdot\psi_0/z . \quad (16)$$

In equations (15) and (16), we have $\psi_0 = R_d(0)/2$ and $b = -\psi_{02} - (\phi_{01}{}^2/\psi_0)$. Moreover, ϕ_{01} and ψ_{02}, are calculated as $\phi_{01} = \mathrm{Im}[R_d'(0)]/2$ and $\psi_{02} = R_d''(0)/2$ [2], where the primes denote derivation with respect to the temporal difference τ and $\mathrm{Im}[.]$ is the imaginary part of the bracketed term. Using equation (5) with equations (6)-(9) and after some algebraic manipulations we obtain

$$\psi_0 = \sigma^2 \quad (17)$$

$$\phi_{01} = \pi\sigma^2 f_{\max} U \sum_{i=1}^{4}[(-1)^{i-1} S_i(\sin a_{\max i} - \sin a_{\min i})\times (\beta_{\max i} - \beta_{\min i} + \sin\beta_{\max i}\cos\beta_{\max i} - \sin\beta_{\min i}\cos\beta_{\min i})] \quad (18)$$

$$\psi_{02} = \frac{\pi^2\sigma^2 f_{\max}{}^2 U}{6}\times \sum_{i=1}^{4}\{S_i[\sin\beta_{\max i}(\cos(2\beta_{\max i})+5) - \sin\beta_{\min i}(\cos(2\beta_{\min i})+5)]\times [s\,\mathrm{in}(2a_{\min i}) - \sin(2a_{\max i}) + 2a_{\min i} - 2a_{\max i}]\} . \quad (19)$$

From equations (17)-(19), we see the fading rate variance b [18], which is essential for determining the LCR and AFD, is analytically calculated for generalized 3-D scattering environments using the ACF, its first and its second derivative at $\tau = 0$. The alternative formulation in [18] required six shape factors.

IV. CONCLUSION

A parameterized diffuse multipath scattering model has been presented, where multi-modal arrival within four sectors has been considered. Those sectors are parametrically defined in order to offer an unlimited flexibility for modeling any 3-D scattering scenario with any arbitrary number of sectors. The PSD has been analytically derived after Fourier transforming the ACF and has been shown to be discontinuous and asymmetric. Finally, for a Rayleigh distributed envelope, the LCR and AFD have been analytically determined using values of the ACF and its derivatives at zero temporal difference.

V. ACKNOWLEDGMENT

This work was accomplished during the first author's employment on the FP7 MC IPLAN project, which provided a partial financial support. Current financial support of the first author is provided by the Institute of Research in Applicable Computing (IRAC) of University of Bedfordshire.

APPENDIX A-DERIVATION OF EQUATIONS (11)-(14)

By taking the Fourier transform of equation (6) we have after some algebraic manipulations

$$F[J_1(\tau)] = 2\sigma^2 S_1 U \times \int_{\beta_{\min 1}}^{\beta_{\max 1}}\int_{a_{\min 1}}^{a_{\max 1}}\int_{-\infty}^{\infty}\cos\beta\exp[-j2\pi\tau(f - f_{\max}\cos\beta\cos a)]d\tau da d\beta \quad (A1)$$

and integration with respect to τ gives

$$F[J_1(\tau)] = 2\sigma^2 S_1 U \int_{\beta_{\min 1}}^{\beta_{\max 1}}\int_{a_{\min 1}}^{a_{\max 1}}\cos\beta\,\delta(f - f_{\max}\cos\beta\cos a) da d\beta \quad (A2)$$

where $\delta(.)$ is the Dirac delta function. We set in equation (A2) $x = \sqrt{f_{\max}}\cos\beta$, $y = \sqrt{f_{\max}}\cos a$ and after some algebraic manipulations we take

$$F[J_1(\tau)] = 2\sigma^2 S_1 U \times \int_{\sqrt{f_{\max}}\cos\beta_{\max 1}}^{\sqrt{f_{\max}}\cos\beta_{\min 1}}\int_{\sqrt{f_{\max}}\cos a_{\max 1}}^{\sqrt{f_{\max}}\cos a_{\min 1}}\frac{x\,\delta(f-xy)}{\sqrt{f_{\max}}\cdot\sqrt{f_{\max} - y^2}\sqrt{f_{\max} - x^2}} dy dx . \quad (A3)$$

The integration in equation (A3) will be for values of x and y where $f = xy$. For any other values of x and y, i.e. $f \neq xy$, the integrand in equation (A3) will be zero. The integration area and the values of x and y where the integrand in equation (A3) is nonzero can be seen in Fig. A1. Integrating with respect to y and after some algebraic manipulations we have

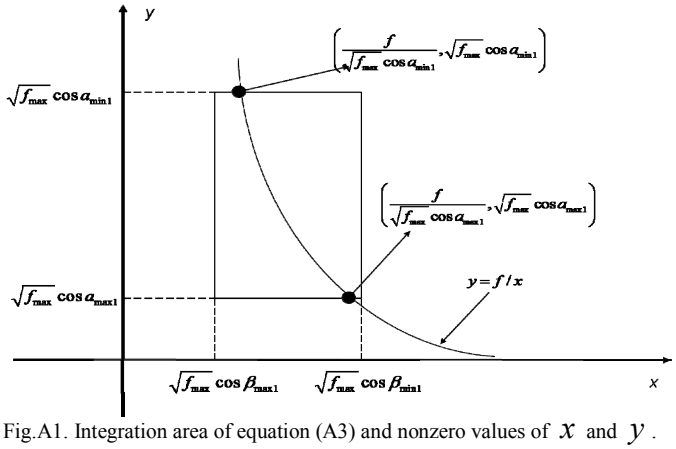

Fig.A1. Integration area of equation (A3) and nonzero values of x and y.

$$F[J_1(\tau)]=\begin{cases}2\sigma^2 S_1 U\int\limits_{\frac{f}{\sqrt{f_{\max}}\cos a_{\max 1}}}^{\frac{f}{\sqrt{f_{\max}}\cos a_{\min 1}}}\dfrac{x/\sqrt{f_{\max}}}{\sqrt{f_{\max}-x^2}\sqrt{f_{\max}x^2-f^2}}dx, \\ f_{\max}\cos a_{\min 1}\cos\beta_{\max 1}\le f\le f_{\max}\cos a_{\max 1}\cos\beta_{\min 1} \\ 2\sigma^2 S_1 U\int\limits_{\frac{f}{\sqrt{f_{\max}}\cos a_{\min 1}}}^{\sqrt{f_{\max}}\cos\beta_{\min 1}}\dfrac{x/\sqrt{f_{\max}}}{\sqrt{f_{\max}-x^2}\sqrt{f_{\max}x^2-f^2}}dx, \\ \max\left(f_{\max}\cos a_{\min 1}\cos\beta_{\max 1}, f_{\max}\cos a_{\max 1}\cos\beta_{\min 1}\right)\le \\ f\le f_{\max}\cos a_{\min 1}\cos\beta_{\min 1} \\ 2\sigma^2 S_1 U\int\limits_{\sqrt{f_{\max}}\cos\beta_{\max 1}}^{\frac{f}{\sqrt{f_{\max}}\cos a_{\max 1}}}\dfrac{x/\sqrt{f_{\max}}}{\sqrt{f_{\max}-x^2}\sqrt{f_{\max}x^2-f^2}}dx, \\ f_{\max}\cos a_{\max 1}\cos\beta_{\max 1}\le f\le \\ \min(f_{\max}\cos a_{\min 1}\cos\beta_{\max 1}, f_{\max}\cos a_{\max 1}\cos\beta_{\min 1}) \\ 2\sigma^2 S_1 U\int\limits_{\sqrt{f_{\max}}\cos\beta_{\max 1}}^{\sqrt{f_{\max}}\cos\beta_{\min 1}}\dfrac{x/\sqrt{f_{\max}}}{\sqrt{f_{\max}-x^2}\sqrt{f_{\max}x^2-f^2}}dx, \\ f_{\max}\cos a_{\max 1}\cos\beta_{\min 1}\le f\le f_{\max}\cos a_{\min 1}\cos\beta_{\max 1} \\ \\ 0, otherwise\end{cases} \tag{A4}$$

The integral limits of x in equation (A4), as well as the Doppler frequency ranges, arise by processing the following inequalities:

a) $f/(\sqrt{f_{\max}}\cos a_{\min 1})\ge\sqrt{f_{\max}}\cos\beta_{\max 1}$, thus $x\ge(f/\sqrt{f_{\max}}\cos a_{\min 1})$ and $f/(\sqrt{f_{\max}}\cos a_{\max 1})\le\sqrt{f_{\max}}\cos\beta_{\min 1}$, thus $x\le(f/\sqrt{f_{\max}}\cos a_{\max 1})$.

b) $f/(\sqrt{f_{\max}}\cos a_{\min 1})\ge\sqrt{f_{\max}}\cos\beta_{\max 1}$, thus $x\ge(f/\sqrt{f_{\max}}\cos a_{\min 1})$ and $f/(\sqrt{f_{\max}}\cos a_{\max 1})\ge\sqrt{f_{\max}}\cos\beta_{\min 1}$, thus $x\le\sqrt{f_{\max}}\cos\beta_{\min 1}$. Moreover, we have by default $f\le f_{\max}\cos a_{\min 1}\cos\beta_{\min 1}$ as $f_{\max}\cos a_{\min 1}\cos\beta_{\min 1}$ is the maximum possible Doppler frequency shift.

c) $f/(\sqrt{f_{\max}}\cos a_{\min 1})\le\sqrt{f_{\max}}\cos\beta_{\max 1}$, thus $x\ge\sqrt{f_{\max}}\cos\beta_{\max 1}$ and $f/(\sqrt{f_{\max}}\cos a_{\max 1})\le\sqrt{f_{\max}}\cos\beta_{\min 1}$, thus $x\le f/(\sqrt{f_{\max}}\cos a_{\max 1})$. Moreover, we have by default $f\ge f_{\max}\cos a_{\max 1}\cos\beta_{\max 1}$ as $f_{\max}\cos a_{\max 1}\cos\beta_{\max 1}$ is the minimum possible Doppler frequency shift.

d) $f/(\sqrt{f_{\max}}\cos a_{\min 1})\le\sqrt{f_{\max}}\cos\beta_{\max 1}$, thus $x\ge\sqrt{f_{\max}}\cos\beta_{\max 1}$ and $f/(\sqrt{f_{\max}}\cos a_{\max 1})\ge\sqrt{f_{\max}}\cos\beta_{\min 1}$, thus $x\le\sqrt{f_{\max}}\cos\beta_{\min 1}$.

The following equation, derived by the author, is valid

$$\int\frac{x/\sqrt{f_{\max}}}{\sqrt{f_{\max}-x^2}\sqrt{f_{\max}x^2-f^2}}dx=\frac{1}{2f_{\max}}arc\sin\frac{2f_{\max}x^2-{f_{\max}}^2-f^2}{{f_{\max}}^2-f^2} \tag{A5}$$

Finally, using equation (A5) in equation (A4) and after some algebraic manipulations, equation (11) arises. Equations (12)-(14) arise by following an exactly similar rationale.

REFERENCES

[1] P. Karadimas and J. Zhang, "A Generalized Analysis of Three-Dimensional Anisotropic Scattering in Mobile Wireless Channels-Part I: Theory," IEEE, Veh. Technol. Conf. (VTC), May 2011.

[2] M. Patzold, "Mobile Fading Channels," Wiley, 2002.

[3] M. J. Gans, "A Power-Spectral Theory of Propagation in the Mobile-Radio Environment," IEEE Trans. Veh. Technol., vol. 21, no. 1, pp. 27-38, Feb. 1972.

[4] T. Aulin, "A Modified Model for the Fading Signal at a Mobile Radio Channel," IEEE Trans. Veh. Technol., vol. 28, no. 3, pp. 182-203, Aug. 1979.

[5] R. H. Clarke and W. L. Khoo, "3-D Mobile Radio Channel Statistics," IEEE Trans. Veh. Technol., vol. 46, no. 3, pp. 798-799, Aug. 1997.

[6] J. D Parsons and A. M. D. Turkmani, "Characterization of Mobile Radio Signals: Model Description," IEE Proc.-I vol. 138, no. 6, pp. 549-556, Dec. 1991.

[7] S. Qu and T. Yeap, "A Three-Dimensional Scattering Model for Fading Channels in Land Mobile Environment," IEEE Trans. Veh. Technol., vol. 48, no. 3, pp. 765-781, May. 1999.

[8] R. Janaswamy, "Radiowave Propagation and Smart Antennas for Wireless Communications," Kluwer Academic Publishers, 2001.

[9] C. Kasparis, P. King and B. G. Evans, "Doppler Spectrum of the Multipath Fading Channel in Mobile Satellite Systems with Directional Terminal Antennas," IET Commun. vol. 1, no. 6, pp. 1089-1094, Dec. 2007.

[10] P. Karadimas, E. D. Vagenas and S. A. Kotsopoulos, "A Small Scale Fading Model with Sectored and Three Dimensional Diffuse Scattering," IEEE Consumer Commun. and Netw. Conf., (CCNC), pp. 943-947, Jan. 2008.

[11] P. Karadimas and S. A. Kotsopoulos, "A Modified Loo Model with Partially Blocked and Three Dimensional Multipath Scattering: Analysis, Simulation and Validation," Springer Wirel. Pers. Commun., vol. 53, pp. 503-528, 2010.

[12] R. Narasimhan and D. C. Cox, "A Generalized Doppler Power Spectrum for Wireless Environments," IEEE Commun. Letters, vol. 3, no. 6, pp. 164-165, June 1999.

[13] X. Zhao, J. Kivinen, P. Vainikainen and K. Skog, "Characterization of Doppler Spectra for Mobile Communications at 5.3 GHz," IEEE Trans. Veh. Technol., vol. 52, no. 1, pp. 14-23, Jan. 2003.

[14] J. Kivinen, X. Zhao and P. Vainikainen, "Empirical Characterization of Wideband Indoor Radio Channel at 5.3 GHz," IEEE Trans. Ant. and Propag., vol. 49, no. 8, pp. 1192-1203, Aug. 2001.

[15] J. M. Morris and J. L. Chang, "Burst Error Statistics of Simulated Viterbi Decoded BFSK and High-Rate Punctured Codes on Fading and Scintillating Channels," IEEE Trans. Commun., vol. 43, no. 2/3/4, pp. 695–700, Feb./Mar./Apr. 1995.

[16] L. F. Chang, "Throughput Estimation of ARQ Protocols for a Rayleigh Fading Channel Using Fade- and Interfade-Duration Statistics," IEEE Trans. Veh. Technol., vol. 40, no. 1, pp. 223–229, Feb. 1991.

[17] T. W. C. Brown and U. M. Ekpe, "When is Clarke's Approximation Valid?" IEEE Ant and Propag. Magazine, vol. 52, no. 3, pp. 171-181, Jun. 2010.

[18] D. G. Valchev and D. Brady, "Three-Dimensional Multipath Shape Factors for Spatial Modeling of Wireless Channels," IEEE Trans. Wirel. Commun., vol. 8, no. 11, pp. 5542-5551, Nov. 2009.

[19] A. Abdi, "On the Utility of Laguere Series for the Envelope PDF in Multipath Fading Channels," IEEE Trans. Inf. Theory, vol. 55, no. 12, pp. 5652-5660, Dec. 2009.